LETTERS

Heterogeneous chemistry in the atmosphere of Mars

Franck Lefèvre[1,2], Jean-Loup Bertaux[2,3], R. Todd Clancy[4], Thérèse Encrenaz[2,5], Kelly Fast[6], François Forget[2,7], Sébastien Lebonnois[2,7], Franck Montmessin[2,3] & Séverine Perrier[2,3]†

Hydrogen radicals are produced in the martian atmosphere by the photolysis of water vapour and subsequently initiate catalytic cycles that recycle carbon dioxide from its photolysis product carbon monoxide[1,2]. These processes provide a qualitative explanation for the stability of the atmosphere of Mars, which contains 95 per cent carbon dioxide. Balancing carbon dioxide production and loss based on our current understanding of the gas-phase chemistry in the martian atmosphere has, however, proven to be difficult[3–5]. Interactions between gaseous chemical species and ice cloud particles have been shown to be key factors in the loss of polar ozone observed in the Earth's stratosphere[6], and may significantly perturb the chemistry of the Earth's upper troposphere[7]. Water-ice clouds are also commonly observed in the atmosphere of Mars[8–10] and it has been suggested previously that heterogeneous chemistry could have an important impact on the composition of the martian atmosphere[3–5,11]. Here we use a state-of-the-art general circulation model together with new observations of the martian ozone layer[12–15] to show that model simulations that include chemical reactions occurring on ice clouds lead to much improved quantitative agreement with observed martian ozone levels in comparison with model simulations based on gas-phase chemistry alone. Ozone is readily destroyed by hydrogen radicals and is therefore a sensitive tracer of the chemistry that regulates the atmosphere of Mars. Our results suggest that heterogeneous chemistry on ice clouds plays an important role in controlling the stability and composition of the martian atmosphere.

One-dimensional, globally averaged models have previously explored the potential impact of heterogeneous chemical processes in the martian atmosphere[3–5,11] but, in the absence of sufficiently strong observational and laboratory evidence, this possibility has remained unproven. Recently, the framework for investigating this issue has improved greatly. The SPICAM ultraviolet spectrometer onboard the Mars-Express spacecraft has for the first time provided global, quasi-continuous observations of the martian ozone layer[12]. Ozone (O_3) is readily destroyed by hydrogen radicals and is therefore a sensitive tracer of the chemistry that regulates the atmosphere of Mars. At the same time, the development of general circulation models (GCM) with interactive photochemistry[16,17] now allows

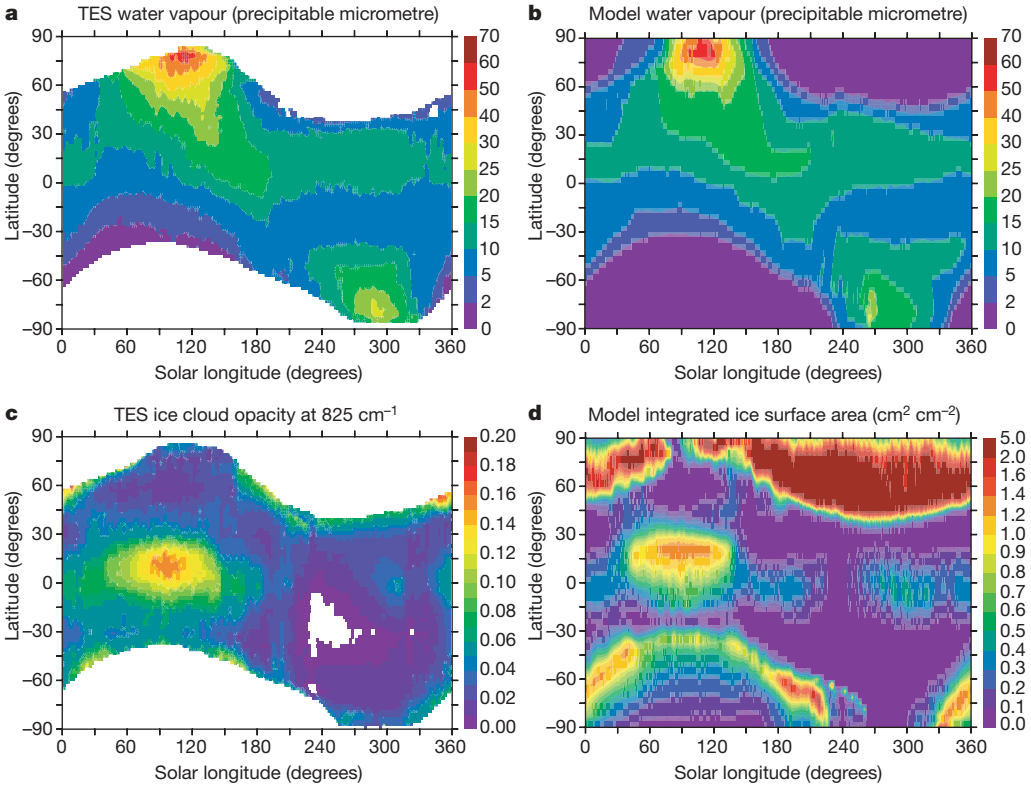

Figure 1 | Observed and simulated seasonal evolution of water vapour and water-ice clouds. **a**, Water vapour column observed by the thermal emission spectrometer[19] on the Mars Global Surveyor, in precipitable micrometres. **b**, Water vapour column calculated by the GCM. **c**, Water-ice cloud opacity at 825 cm^{-1} observed by TES. **d**, Vertically integrated surface area of water-ice cloud calculated by the GCM, in $cm^2\ cm^{-2}$. Solar longitude (L_s) is used to specify seasons on Mars, and is 0° at the northern vernal equinox and 270° at northern winter solstice.

[1]UPMC Univ. Paris 06, Service d'Aéronomie, Paris F-75005, France. [2]CNRS/INSU, France. [3]Université Versailles St-Quentin, Service d'Aéronomie, Verrières-le-Buisson F-91371, France. [4]Space Science Institute, 4750 Walnut Street, Suite 205, Boulder, Colorado 80301, USA. [5]LESIA, Observatoire de Paris, F-92195 Meudon, France. [6]Planetary Systems Laboratory, Code 693, NASA Goddard Space Flight Center, Greenbelt, Maryland 20771, USA. [7]UPMC Univ. Paris 06, Laboratoire de Météorologie Dynamique, Paris F-75005, France. †Present address: Direction Générale pour l'Armement, Bagneux F-92220, France.

observational data to be analysed at the same level of sophistication as for terrestrial studies. To re-evaluate our quantitative understanding of martian photochemistry, we carried out a stringent comparison between ozone predicted by the GCM with photochemistry developed at Laboratoire de Météorologie Dynamique[16] (LMD) and the SPICAM data collected during more than one martian year. Also included in our analysis are Earth-based ozone measurements made at various seasons before the Mars-Express mission, from the Hubble Space Telescope[13,14] (HST) and the NASA Infrared Telescope Facility (IRTF)[15].

Because water vapour is the source of ozone-destroying HO_x species, it is important to ensure first that the martian water cycle is simulated correctly by the GCM. We therefore adjusted the parameters of the microphysical scheme used in the model[18] to obtain optimal quantitative agreement with the seasonal evolution of H_2O given by the Thermal Emission Spectrometer[19] (TES) onboard the Mars Global Surveyor (Fig. 1a, b; see also the Supplementary Information). The model also provides a good match to the equatorial cloud belt usually observed between solar longitudes $L_s = 30°$–$150°$ during the colder aphelion season[8,19] (Fig. 1c, d). At high latitudes, the GCM predicts large ice surface areas in the polar hoods that start to form in late summer. This hypothesis is consistent with the strong opacities measured in the polar hoods at visible[9] and ultraviolet[10] wavelengths. TES data obtained at the edge of the seasonal CO_2 caps also support this result.

The model ozone is compared with observations in Fig. 2. At high latitudes of both hemispheres, SPICAM indicates a marked seasonal evolution which is anti-correlated with the amount of water vapour: the largest O_3 columns are found in the dry winter/spring polar vortices, whereas O_3 is close to zero in summer. This behaviour is qualitatively well reproduced by our first GCM simulation, which considers only the gas-phase photochemistry. However, rigorous comparison with SPICAM shows significant quantitative differences. In the latitude band 70° N–90° N (Fig. 2a), the model predicts ozone loss that is too fast in early spring ($L_s = 10°$–$40°$) and underestimates the column by about 10 μm atm. In late summer ($L_s = 150°$–$180°$), the O_3 increase is too slow in the model, which results in amounts that are lower by a factor of almost three relative to observations. This

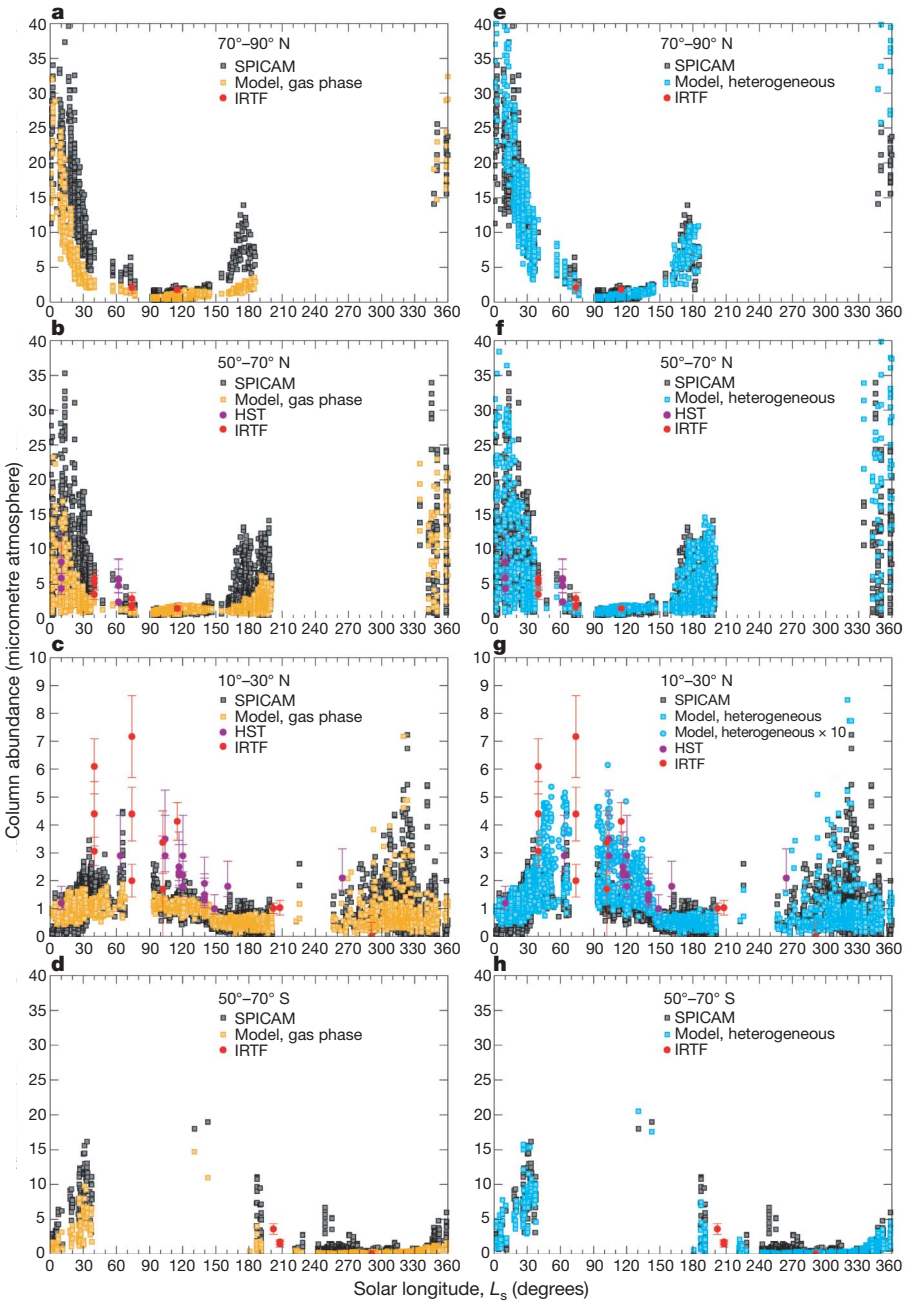

Figure 2 | Observed and simulated seasonal evolution of martian ozone. The GCM ozone columns are compared with those measured from SPICAM, the HST[13,14], and the IRTF[15]. In the left column, the model only considers gas-phase photochemical reactions. The right column incorporates the heterogeneous loss of HO_x on water-ice clouds. Blue circles in **g** represent the O_3 columns obtained when the cloud surface area is multiplied by 10 for $L_s = 30°$–$150°$. In all panels model values are plotted over SPICAM data points. A unit of 1 micrometre atmosphere is a column abundance of 2.689×10^{15} molecules cm^{-2}, or 0.1 Dobson unit. Note the change in vertical scale at 10° N–30° N. Error bars indicate uncertainties in the individual measurements.

bias is confirmed at 50° N–70° N (Fig. 2b) and 50° S–70° S (Fig. 2d): although the GCM partially reproduces the strong day-to-day ozone variability related to the presence of the polar vortex edge in these latitude bands[16], the peak O_3 values calculated in early spring and around autumn equinox are underestimated relative to SPICAM.

The ozone annual cycle at low latitudes is of much more limited amplitude. At 10° N–30° N (Fig. 2c), it is characterized by a broad seasonal maximum centred on Mars aphelion ($L_s = 71°$), and by strong day-to-day variability in winter. The gas-phase-only GCM reproduces this behaviour qualitatively well. Near aphelion, the ozone enhancement results from the decrease in water vapour saturation altitude and the subsequent build-up of a seasonal ozone layer above 30 km altitude[16,20,21]. In winter, deformations of the O_3-rich polar vortex sporadically bring large quantities to mid-to-low latitudes, explaining the fast changes observed by SPICAM. However, although there is rather large scatter in the observational data, it is evident that the GCM underestimates the O_3 values generally detected in the aphelion season.

The fact that the gas-phase-only model underestimates ozone amounts during opposite seasons at high and low latitudes seems to be a robust result. First, both water vapour and dust[22] fields are constrained by TES observation; thus we cannot invoke a possible overestimation of H_2O, or an unrealistic amount of dust that might affect the photolysis rate calculations, to explain the disagreement. Second, the GCM ozone columns are coincident with SPICAM observations; local effects induced by topography, local time or three-dimensional transport are therefore taken into account. Third, we explored the solutions offered by current uncertainties in the photochemical and gas-phase kinetics data of martian interest; changing these parameters in the limits allowed by laboratory and field evidence on Earth does not allow a significant increase in ozone[16]. Finally, the ozone profiles measured by SPICAM above 30 km do not indicate an underestimation by the model at high latitudes, or at low latitudes near aphelion[21]. Therefore, if the discrepancy with observed ozone columns is the result of a missing process in the gas-phase model, then (1) it must be essentially confined below 30 km, (2) at high latitudes, it must be active only in or near the polar vortex, and (3) at low latitudes, it must be especially efficient in the aphelion season and no later than $L_s = 150°$. Interestingly, these three conditions go against the observed climatology of atmospheric dust[12,19], which tends to exclude heterogeneous reactions on dust as good candidates to explain the SPICAM data. On the other hand, these constraints are well satisfied by water-ice clouds, and we therefore introduced heterogeneous chemistry on clouds in a second GCM simulation. Heterogeneous reaction rates are proportional to the available surface area and to their surface reaction probability, γ. To limit the uncertainties, we made the conservative choice of considering only the reactions of martian interest for which γ has been identified and measured in the laboratory. This led us to implement only the uptake of HO_2 and OH on water-ice, adopting $\gamma_{HO_2} = 0.025$ and $\gamma_{OH} = 0.03$ (ref. 23).These values are those currently recommended for terrestrial studies[24].

At $L_s = 30°$, the HO_x uptake on the northern polar hood multiplies the ozone abundance by a factor of about four in the polar vortex (Fig. 3). Heterogeneous chemistry brings the model into excellent quantitative agreement with SPICAM throughout the springtime period (Fig. 2e, f), does not degrade the satisfying results already obtained with the gas-phase experiment in early summer, and reproduces well the rapid growth in ozone after $L_s = 150°$. As a consequence of the larger O_3 latitudinal gradients, the variability observed at 50° N–70° N and 50° S–70° S is better reproduced, and the maximum values predicted in the northern hemisphere (30–40 μm atm) are more consistent both with SPICAM and with the early observations of Mariner 9 (ref. 25).

At low latitudes, introducing heterogeneous chemistry on the aphelion cloud belt doubles the amount of ozone at $L_s = 70°$ (Fig. 3),

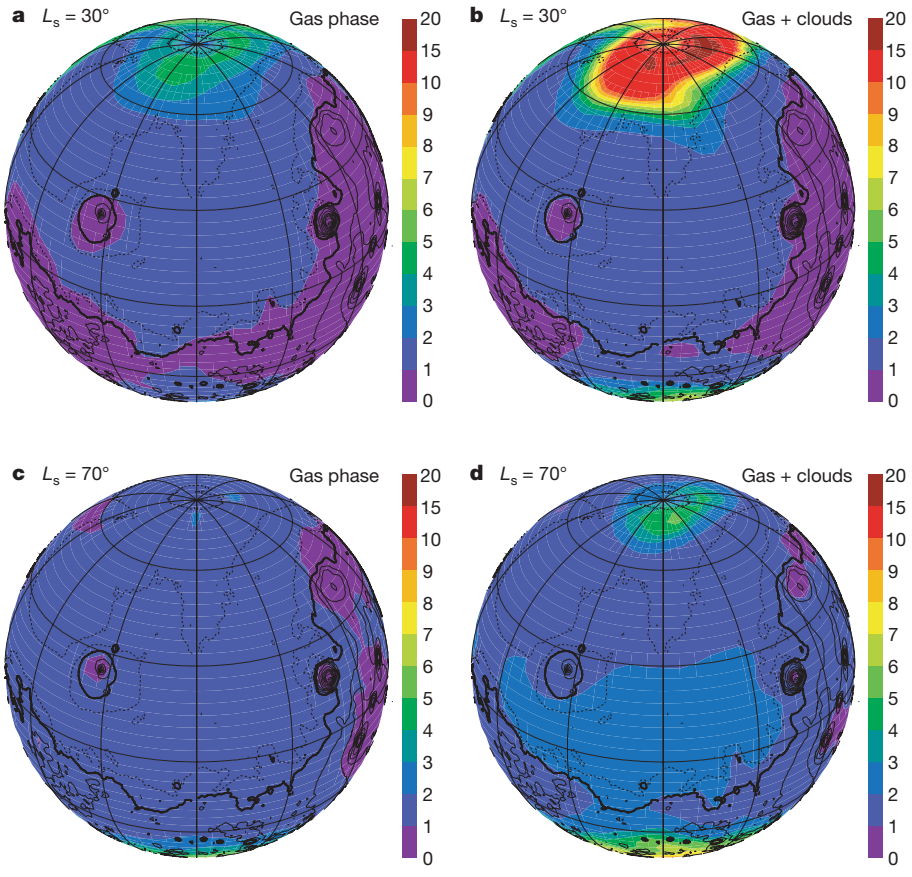

Figure 3 | Synoptic distribution of O_3 column (micrometre atmosphere) calculated in northern spring and at aphelion. **a**, **c**, Gas-phase-only photochemical scheme; **b**, **d**, with heterogeneous loss of HO_x on water-ice clouds. The observer is facing the 180° meridian at local noon, and the black contours correspond to Mars topography at 2-km intervals.

which allows a more accurate description of the observed seasonal maximum. However, the largest values detected by SPICAM and from Earth (4 to 7 μm atm at $L_s = 74°$, 3 to 7 μm atm for $L_s = 100$–$120°$) still seem outstanding. We investigated this issue by multiplying the predicted cloud surface area by a factor of 10 to account for uncertainties in the modelled ice particle number density, radius, shape and sub-grid-scale inhomogeneities. This sensitivity experiment shows a further doubling in ozone which allows the model to reach virtually all the peak values measured during the aphelion season (Fig. 2g). Heterogeneous chemistry seems, therefore, to have the potential to explain the full amplitude of the O_3 column variations observed in this season. Furthermore, this result is obtained with modelled CO values that also match the observations (see Supplementary Information).

A further hint of the proposed mechanism is provided by the Earth-based measurements[26,28–30] of Mars atmospheric H_2O_2, the temporary HO_x reservoir produced by the reaction between two HO_2 radicals, also thought to be the main oxidant of the martian surface. Figure 4 shows that the seasonal variation of H_2O_2 at low latitudes is reasonably well reproduced by the gas-phase GCM, except at $L_s = 112°$, when the model prediction exceeds the observed upper limit[26] by a factor of three. Consistent with what is found for ozone, introducing the HO_x uptake on the aphelion cloud belt into the model largely reduces that discrepancy. We do not exclude the possibility that other unknown or poorly quantified chemical processes might diminish H_2O_2 and have an impact on ozone. It must be emphasized, however, that heterogeneous chemistry as introduced in the GCM improves the agreement with measurements of both O_3 and H_2O_2 without violating current laboratory constraints. This result suggests that water-ice clouds play an important role in the composition and evolution of the martian atmosphere. As the same processes are believed to occur on cirrus clouds on Earth, it also sheds new light on the role of Mars as a natural laboratory for better understanding the chemistry of our own atmosphere.

METHODS SUMMARY

The LMD GCM was integrated at a resolution of 3.75° latitude × 5.625° longitude, on 32 vertical levels from the ground up to about 120 km. In the simulations presented here the model uses a prescribed distribution of atmospheric dust constructed from the sequential assimilation of TES data[22]. This dust field is three-dimensional, evolves with time and reproduces the TES observations of martian years 24 and 25 (before the global dust storm). The photochemical code implemented in the GCM is an evolution of the model extensively described previously[16], with updated kinetics and photochemical data[24].

In Fig. 1 the GCM is compared with water vapour data obtained from a recent re-analysis of the TES retrieval. The revised TES algorithm results in a reduction in derived H_2O abundances of about 30% when the instrument was in its lower resolution mode (M. Smith, personal communication). This correction improves the agreement with corresponding Mars-Express water vapour data[27], and also reduces the year-to-year variability that was present in the original TES retrievals[19].

SPICAM data were collected between January 2004 ($L_s = 331°$ of martian year 26) and June 2006 ($L_s = 68°$ of martian year 28). The uncertainty on the ozone column is estimated[12] to be 10–15%. When compared with SPICAM, the GCM ozone column was extracted for each observation from the closest grid point with a time difference less than 1 h. To avoid the regions where fast O_3 variations may occur near the day–night terminator, we excluded from the analysis the measurements obtained at solar zenith angles larger than 80°. Ozone data from the HST and from the IRTF were obtained for 1995–2003 and 1988–2003, respectively.

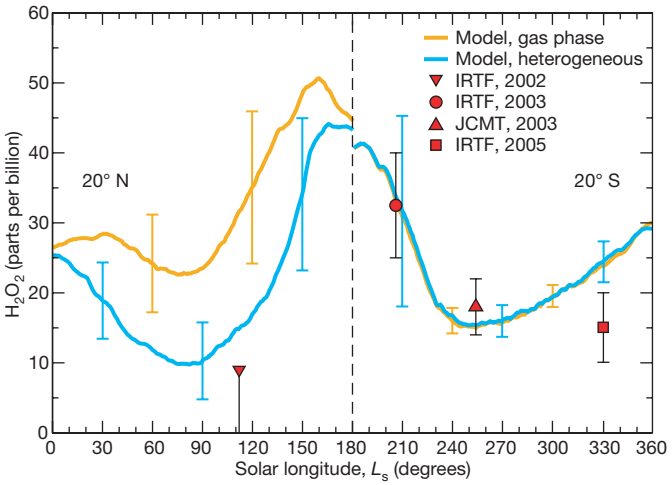

Figure 4 | Observed and simulated seasonal evolution of martian hydrogen peroxide (H_2O_2). Results are plotted in parts per billion (10^{-9}) at latitudes corresponding to the approximate subsolar point of the observations: 20° N between $L_s = 0°$ and 180°, and 20° S between $L_s = 180°$ and 360°. Measurements were obtained with the IRTF[26,28,29] and the James Clerk Maxwell Telescope[30] (JCMT). The value at $L_s = 112°$ is an upper limit in the 10°–40° N band. The orange and blue curves represent the H_2O_2 abundances calculated by the model on the latitude circle, without and with consideration of heterogeneous loss of HO_x on water-ice clouds. Errors bars represent variability (2σ).

Received 21 November 2007; accepted 27 May 2008.

1. McElroy, M. B. & Donahue, T. M. Stability of the Martian atmosphere. *Science* **177,** 986–988 (1972).
2. Parkinson, T. D. & Hunten, D. M. Spectroscopy and aeronomy of O_2 on Mars. *J. Atmos. Sci.* **29,** 1380–1390 (1972).
3. Atreya, S. K. & Blamont, J. E. Stability of the Martian atmosphere: possible role of heterogeneous chemistry. *Geophys. Res. Lett.* **17,** 287–290 (1990).
4. Atreya, S. K. & Gu, Z. G. Stability of the Martian atmosphere: Is heterogeneous catalysis essential? *J. Geophys. Res.* **99,** 13133–13145 (1994).
5. Krasnopolsky, V. A. Photochemistry of the Martian atmosphere: Seasonal, latitudinal, and diurnal variations. *Icarus* **185,** 153–170 (2006).
6. Solomon, S. Stratospheric ozone depletion: A review of concepts and history. *Rev. Geophys.* **37,** 275–316 (l999).
7. Jaeglé, L. *et al.* Photochemistry of HO_x in the upper troposphere at northern midlatitudes. *J. Geophys. Res.* **105,** 3877–3892 (2000).
8. Clancy, R. T. *et al.* Water vapor saturation at low altitudes around Mars aphelion: A key to Mars climate? *Icarus* **122,** 36–62 (1996).
9. Akabane, T., Iwasaki, K., Saito, Y. & Narumi, Y. Martian late-northern-winter polar hood opacities and non-visibility of a surface cap: 1975 and 1990 observations. *Astron. Astrophys.* **277,** 302–308 (1993).
10. Mateshvili, N. *et al.* Martian ice cloud distribution obtained from SPICAM nadir UV measurements. *J. Geophys. Res.* **112,** doi:10.1029/2006JE002827 (2007).
11. Anbar, A. D., Leu, M. T., Nair, H. A. & Yung, Y. L. Adsorption of HO_x on aerosol surfaces: Implications for the atmosphere of Mars. *J. Geophys. Res.* **98,** 10933–10940 (1993).
12. Perrier, S. *et al.* Global distribution of total ozone on Mars from SPICAM/MEX UV measurements. *J. Geophys. Res.* **111,** doi:10.1029/2006JE002681 (2006).
13. Clancy, R. T. *et al.* Mars ozone measurements near the 1995 aphelion: Hubble space telescope ultraviolet spectroscopy with the faint object spectrograph. *J. Geophys. Res.* **101,** 12777–12783 (1996).
14. Clancy, R. T., Wolff, M. J. & James, P. B. Minimal aerosol loading and global increases in atmospheric ozone during the 1996–1997 Martian northern spring season. *Icarus* **138,** 49–63 (1999).
15. Fast, K. *et al.* Ozone abundances on Mars from infrared heterodyne spectra I: Acquisition, retrieval, and anticorrelation with water vapor. *Icarus* **181,** 419–431 (2006).
16. Lefèvre, F., Lebonnois, S., Montmessin, F. & Forget, F. Three-dimensional modeling of ozone on Mars. *J. Geophys. Res.* **109,** doi:10.1029/2004JE002268 (2004).
17. Moudden, Y. & McConnell, J. C. Three-dimensional on-line chemical modeling in a Mars general circulation model. *Icarus* **188,** 18–34 (2007).
18. Montmessin, F., Forget, F., Rannou, P., Cabane, M. & Haberle, R. M. Origin and role of water ice clouds in the Martian water cycle as inferred from a general circulation model. *J. Geophys. Res.* **109,** doi:10.1029/2004JE002284 (2004).
19. Smith, M. D. Interannual variability in TES atmospheric observations of Mars during 1999–2003. *Icarus* **167,** 148–165 (2004).
20. Clancy, R. T. & Nair, H. Annual (perihelion–aphelion) cycles in the photochemical behavior of the global Mars atmosphere. *J. Geophys. Res.* **101,** 12785–12790 (1996).
21. Lebonnois, S. *et al.* Vertical distribution of ozone on Mars as measured by SPICAM/Mars-Express using stellar occultations. *J. Geophys. Res.* **111,** doi:10.1029/2005JE002643 (2006).
22. Montabone, L., Lewis, S. R. & Read, P. L. Interannual variability of Martian dust storms in assimilation of several years of Mars Global Surveyor observations. *Adv. Space Res.* **36,** 2146–2155 (2005).
23. Cooper, P. L. & Abbatt, J. P. Heterogeneous interactions of OH and HO_2 radicals with surfaces characteristic of atmospheric particulate matter. *J. Phys. Chem.* **100,** 2249–2254 (1996).

24. Sander, S. P. *et al. Chemical Kinetics and Photochemical Data for Use in Atmospheric Studies, Evaluation Number 15.* JPL Publ. 06–2 (Jet Propulsion Lab., Pasadena, 2006).
25. Barth, C. A. *et al.* Mariner 9 ultraviolet spectrometer experiment: Seasonal variation of ozone on Mars. *Science* **179,** 795–796 (1973).
26. Encrenaz, T. *et al.* A stringent upper limit of the H_2O_2 abundance in the Martian atmosphere. *Astron. Astrophys.* **396,** 1037–1044 (2002).
27. Fouchet, T. *et al.* Martian water vapor: Mars Express PFS/LW observations. *Icarus* **190,** 32–49 (2007).
28. Encrenaz, T. *et al.* Hydrogen peroxide on Mars: Evidence for spatial and seasonal variations. *Icarus* **170,** 424–429 (2004).
29. Encrenaz, T. *et al.* Simultaneous mapping of H_2O and H_2O_2 on Mars from infrared high-resolution imaging spectroscopy. *Icarus* **195,** 547–556 (2008).
30. Clancy, R. T., Sandor, B. J. & Moriarty-Schieven, G. H. A measurement of the 362 Ghz absorption line of Mars atmospheric H_2O_2. *Icarus* **168,** 116–121 (2004).

Supplementary Information is linked to the online version of the paper at www.nature.com/nature.

Acknowledgements Much of this work was done while F.L. was on leave from CNRS at the Instituto de Astrofísica de Andalucía (Granada, Spain). We thank M. Smith, who provided the TES data.

Author Information Reprints and permissions information is available at www.nature.com/reprints. Correspondence and requests for materials should be addressed to F.L. (franck.lefevre@aero.jussieu.fr).